[submitted to Mol. Cryst. Liq. Cryst]

INHOMOGENEOUS TRANSLATIONAL DIFFUSION IN POLYMER-DISPERSED LIQUID CRYSTALS: MONTE CARLO SIMULATIONS OF NMR SPECTRA

CESARE CHICCOLI,[a] PAOLO PASINI,[a] GREGOR SKAČEJ,[b] CLAUDIO ZANNONI,[c] and SLOBODAN ŽUMER[b]

[a]Istituto Nazionale di Fisica Nucleare, Sezione di Bologna, Via Irnerio 46, I-40126 Bologna, Italy; [b]Physics Department, University of Ljubljana, Jadranska 19, SI-1000 Ljubljana, Slovenia; [c]Dipartimento di Chimica Fisica ed Inorganica, Università di Bologna, Viale Risorgimento 4, I-40136 Bologna, Italy

The methodology for calculating ^{2}H NMR spectra, starting from Monte Carlo simulations of nematic droplets, is briefly reviewed. We focus on effects of translational diffusion, in particular on inhomogeneities in molecular motion close to the droplet wall, and establish a correspondence with the resulting NMR spectra for radial and bipolar droplets. Finally, we also present spectra for samples containing several bipolar droplets with randomly oriented droplet symmetry axes.

Keywords: polymer-dispersed liquid crystals; deuterium NMR; Monte Carlo simulations; translational diffusion

INTRODUCTION

Polymer-dispersed liquid crystals (PDLC) have over the past decade become important both for technological applications and for studies of liquid crystalline ordering in a strongly confined environment.[1] Depending on the polymer matrix and on preparation methods, different structures

can be observed inside nematic droplets. The radial for homeotropic surface anchoring[2,3] and the bipolar for planar anchoring[2,3,4] (Fig. 1) are the most known. Experimentally, various techniques have been applied to study these complex systems, for example calorimetry, light scattering, polarized light microscopy, and deuterium (^{2}H) NMR.[1–4] On the other hand, theoretical approaches based on elastic continuum theory[1] and computer simulations — predominantly of Monte Carlo (MC) type[5] — have been widely used to study PDLC and to express the results in form of experimental observables like polarized light textures or ^{2}H NMR spectra.[6–8]

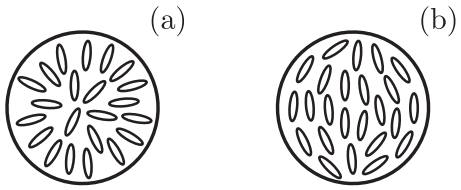

FIGURE 1 Molecular ordering inside a PDLC droplet at a nematic temperature (depicted schematically); (a) radial, (b) bipolar structure.

Recently, we have developed a methodology for employing the numerical output from MC simulations to calculate ^{2}H NMR spectra, which has been demonstrated to be appropriate also in presence of significant molecular motion, including fluctuations of molecular long axes and molecular translational diffusion.[9,10] However, in a thin layer close to the polymer substrate the diffusive motion is slowed down significantly, as seen in some experimental studies.[11,12] The present paper deals with the simulations of this effect in bipolar and radial droplets, applying the methodology presented in Refs. [9,10] and described briefly in the next Section. The resulting spectra are then presented and interpreted qualitatively in the last two Sections.

MONTE CARLO SIMULATIONS AND CALCULATION OF NMR SPECTRA

To simulate the nematic liquid crystal we use a model system suggested by Lebwohl and Lasher decades ago:[13] nematic molecules or close-packed molecular clusters containing up to 100 molecules are represented by particles ("spins") which are arranged into a simple cubic lattice, but can rotate freely. Denoting the orientation of the jth particle by a unit vector

$\mathbf{u}_j$ and the interaction strength constant by ϵ, in absence of external fields the total interaction energy of N particles can be written as

$$U_N = -\frac{\epsilon}{2} \sum_{\langle i<j \rangle} \left[3 \left(\mathbf{u}_i \cdot \mathbf{u}_j \right)^2 - 1 \right], \tag{1}$$

favoring parallel molecular alignment. The sum in Eq. (1) goes over nearest neighbors only. The NMR spectrometer magnetic field is assumed to be sufficiently weak not to affect the molecular organization inside the system. The droplet is then modeled by carving a sphere of a given radius (R) from the cubic lattice, with an additional surface layer of "ghost" particles with fixed orientations imposing radial or bipolar boundary conditions. For simplicity, the interaction constants ϵ for the nematic-nematic and nematic-"ghost" interaction are here chosen to be equal, which implies that surface anchoring is rather strong.[10]

The MC calculations have been performed using the Metropolis algorithm, as described in detail in Ref. [6]. After equilibration, 1024 particle configurations were stored and used as input for the calculation of NMR spectra.[9] The number of particles in the simulation was set to 5832 and the number of "ghosts" to 1352.

From the experimental point of view, ^{2}H NMR is a convenient method for investigating PDLC [2,4,14–16] since — in contrast to optical methods — it is applicable to submicron droplets and it only yields information on the deuterated liquid crystal molecules. It reflects both its static (director field) and dynamic properties (molecular fluctuations and diffusion). A bulk sample of a deuterated nematic in the isotropic phase yields a single narrow line positioned in the spectrum at Zeeman frequency ω_Z, with a width below 100 Hz. In the nematic phase, however, quadrupolar interactions between deuterons and the electric field gradient (EFG) of the C–^{2}H bonds result in a frequency splitting. Assuming that the effective EFG tensor is uniaxial and that biaxiality in molecular ordering is negligible, this splitting is given by [1,17]

$$\omega_Q = \pm \, \delta\omega_Q \, S \left(\frac{3\cos^2\theta - 1}{2} \right). \tag{2}$$

Here θ denotes the angle between the nematic director $\mathbf{n}$ and the NMR spectrometer magnetic field $\mathbf{B_0}$, S stands for the usual uniaxial scalar order parameter,[18] and $\delta\omega_Q$ is the quadrupolar coupling constant (with $\delta\omega_Q/2\pi$ of the order of several 10 kHz). In any confined system both $\mathbf{n}$ and S are position ($\mathbf{r}$) dependent, therefore each type of boundary conditions reflects in spectra via the $\omega_Q = \omega_Q(\mathbf{r})$ dependence and the subsequent average of the local domain contributions over the distribution of domains.

To include dynamic effects when spectra are calculated, it is convenient to apply a semiclassical approach with the time-dependent deuteron spin Hamiltonian.[17] This approach consists of generating the relaxation function

$$G(t) = \exp(i\omega_Z t)\Big\langle \exp\left[i\int_0^t \Omega_Q^j(t')\,dt'\right]\Big\rangle_j, \tag{3}$$

with $\Omega_Q^j(t) = \pm\,\delta\omega_Q\left[3\,(\mathbf{u}_j\cdot\mathbf{B_0}/B_0)^2-1\right]/2$, $\mathbf{u}_j = \mathbf{u}_j(t)$ standing for the "instantaneous" orientation of the jth particle, and $\langle ...\rangle_j$ denoting an ensemble average over all particles in the sample. Once the $G(t)$ function is generated, the NMR spectrum $I(\omega)$ is calculated by performing a Fourier transform $I(\omega) = \int \exp(i\omega t)\,G(t)\,dt$. In our simulation the orientations $\mathbf{u}_j$ are obtained from the 1024 MC configurations, which reproduces the effect of fluctuating molecular long axes. Translational diffusion, however, is simulated by an isotropic random walk process on the lattice. Within this process, in every diffusion step each particle "jumps" to a randomly chosen neighbor lattice site, thereby acquiring the instantaneous orientation $\mathbf{u}_j$ at the new position.

As suggested by experimental results, in a thin subsurface layer molecular diffusive motion is hindered, which results in a significant reduction of the effective diffusion constant D (even by a factor of 3×10^3)[11,12]. In the simulation, the thickness of this layer was set to roughly one particle dimension (up to ~ 5 nm), thereby leaving 1608 particles (out of 5832) in the subsurface region. Then the rate of diffusive moves within this region was reduced and the same reduction factor was assumed also for moves entering or leaving the surface layer. Note also that since nematics are anisotropic liquids, the process of translational diffusion is anisotropic. Consequently, the ratio of the diffusion constants measured along and perpendicular to the director $\mathbf{n}$ can typically be of the order of ~ 2.[2,18] However, since we are primarily interested in qualitative features of spectra, for simplicity the diffusive process is assumed to be isotropic. Some preliminary tests with anisotropic diffusion show that qualitatively our results do not change.

Quantitatively, the degree of diffusional averaging can be determined by calculating the value of the dimensionless parameter $e = \delta\omega_Q R^2/12\pi D$.[2] For $e \gg 1$ the average molecular displacement $\sqrt{6Dt_0}$ within the characteristic NMR time scale $t_0 \sim \delta\omega_Q^{-1}$ is much smaller than the characteristic system size (droplet radius R). Consequently, $\omega_Q(\mathbf{r})$ does not change significantly on the t_0 time scale, which corresponds to the "static" (no-diffusion) limit. On the other hand, $e \ll 1$ with $\sqrt{6Dt_0} \gg R$ corresponds to the fast diffusion limit where NMR spectra are motionally av-

eraged. Consequently, for given D and $\delta\omega_Q$ diffusive effects are important in smaller droplets, where the director $\mathbf{n}$ and ω_Q vary significantly over shorter distances. In cases we claim to correspond to the fast diffusion limit in the simulation, we have $e \approx 0.56$. Despite the condition $e \ll 1$ is still far from being fulfilled, effects of diffusion are already significant, while a further increase of the diffusion rate would only decrease the line widths. For $\delta\omega_Q \approx 2\pi \times 40$ kHz and $D \approx 4 \times 10^{-11}$ m^2/s, $e \approx 0.56$ can be expressed in terms of the droplet radius, indicating that spectra of droplets with radii below 60 nm are already diffusion-averaged. With a single particle in the simulation representing up to 100 nematic molecules, the maximum droplet radius that we can simulate also approaches 60 nm. Therefore, we are always in the fast diffusion regime and the no-diffusion spectra will only be given for a better comprehension. Further, since the droplet is rather small and a significant portion ($\approx 28\%$) of particles lies in the surface layer, a substrate-induced slowdown in translational diffusion is expected to be clearly visible. For any further details the reader is referred to our previous papers.[9,10]

SPECTRA: RADIAL AND BIPOLAR DROPLET

First consider the droplet with radial boundary conditions at $T^* = k_B T/\epsilon = 0.8$, which assures the existence of the nematic phase. In the radial case with homeotropic surface anchoring all particles are directed radially from the droplet center, while in the center there is a rather small defect core (Fig. 1).[19] Ignoring translational diffusion, the spectrum consists of two asymmetric peaks and is similar to the Pake-type powder pattern [Fig. 2 (a)], characteristic for any orientationally isotropic molecular distribution.[17] Note that the total width of the spectrum is less than $2\,\delta\omega_Q$, which is a consequence of fluctuating molecular long axes. From the positions of the two peaks known to be situated at $\pm\frac{1}{2}\delta\omega_Q S$, one can estimate the value of the scalar order parameter S and compare it with the results obtained directly from MC data.[9,10] To smoothen the rather noisy spectra, we have performed a convolution with a Gaussian kernel whose width was rather large ($0.04\,\delta\omega_Q$).

Allowing now particles to diffuse rapidly throughout the whole droplet, the double-peaked pattern collapses into a single peak centered at zero quadrupolar splitting, as shown in Fig. 2 (c). Generally, in the fast diffusion limit the spectrum is expected to consist of two well-defined symmetric lines located at $\langle\omega_Q\rangle$, where $\langle ...\rangle$ denotes an average over the dif-

fusive motion $\mathbf{r}(t)$ of a given particle within the characteristic NMR time scale.[2,17] Since for any isotropic orientational particle distribution we have $\langle\omega_Q\rangle = 0$, in the spectrum there is a single peak at zero splitting.

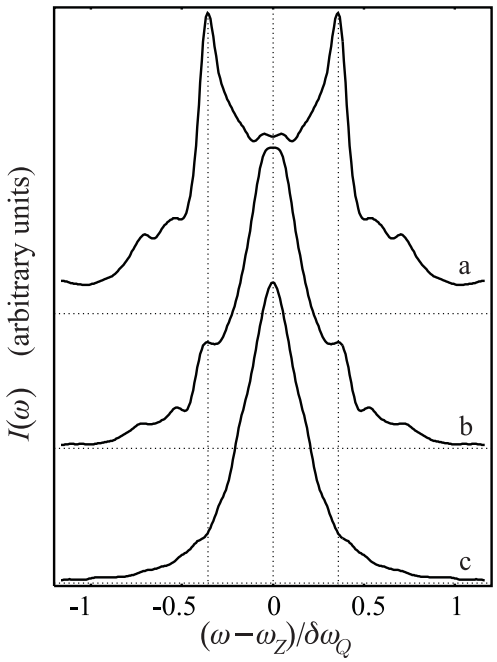

FIGURE 2 Spectra of the radial droplet at $T^* = 0.8$: no diffusion (a), fast diffusion: inhomogeneous (b) and homogeneous (c). Everywhere spectra are normalized so as to yield the same peak height.

If surface inhomogeneities in translational diffusion are taken into account, in the spectra — apart from the diffusion-averaged central peak — there are now two well-pronounced peaks at $\pm 0.36\,\delta\omega_Q$, plus some additional signal at frequencies $0.4\,\delta\omega_Q < |\omega_Q| < 0.8\,\delta\omega_Q$. The spectrum displayed in Fig. 2 (b) was calculated for $D_b/D_s = 3 \times 10^3$, where D_b and D_s are the effective diffusion constants in the bulk and in the surface layer.[11] Since the ratio D_b/D_s is rather large, in the surface layer containing 28% of molecules there is almost no diffusive motion in comparison to the droplet core. Therefore, it is possible to understand the spectrum depicted in Fig. 2 (b) as a weighted superimposition of a diffusion-averaged contribution originating from the droplet core — the central peak — and of an underlying Pake-type pattern originating from the surface layer, affected only negligibly by the slow diffusion. Then from peak positions $\pm 0.36\,\delta\omega_Q$ one can roughly estimate the value of the order parameter in

the surface layer, which yields $S \approx 0.72$. For that layer the S-profiles calculated from MC data give $S \approx 0.80$ [10] and the agreement is sufficiently good.

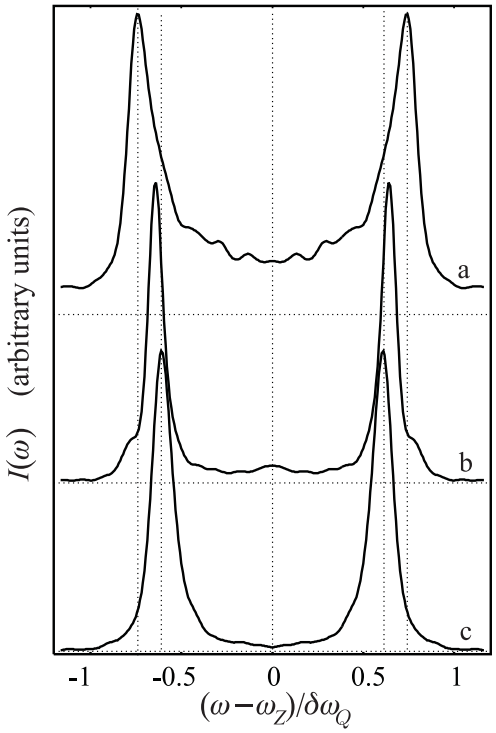

FIGURE 3 Spectra of the bipolar droplet at $T^* = 0.8$: no diffusion (a), fast diffusion: inhomogeneous (b) and homogeneous (c).

In the bipolar case, surface anchoring is planar and in the droplet core most particles are aligned along a given direction, determined by the bipolar symmetry axis (Fig. 1). Where the axis intersects the droplet surface, there are two defects at the "poles" of the droplet. In our case the bipolar axis was chosen parallel to the spectrometer magnetic field. Consequently, in the no-diffusion regime the spectrum consists of two lines positioned approximately at $\pm\delta\omega_Q S$ [see Fig. 3 (a)]. Again, one can deduce the value of S from the peak positions. Considering the homogeneous fast diffusion case, the two lines in the spectrum move towards a lower splitting $|\langle\omega_Q\rangle|$ [Fig. 3 (c)]. This is expected since not all particles are exactly parallel to the spectrometer field and thus yield smaller $|\omega_Q|$ contributions when the average $\langle ...\rangle$ is performed. If, however, diffusion is inhomogeneous [again with $D_b/D_s = 3 \times 10^3$; Fig. 3 (b)], the two main peaks in the spectrum move slightly apart, but do not exceed the initial splitting obtained in the

diffusionless case. The diffusive paths of particles now mostly avoid the surface region where the curvature of the director field is strongest and, consequently, the deviations from the maximum $|\omega_Q|$ are largest, which explains the re-positioning of the main peaks. Further, there are two additional "shoulders" positioned at a splitting slightly larger than that corresponding to the main peaks. These "shoulders" originate from the diffusion-unaffected surface layer, especially from particles aligned almost along the spectrometer field. Note that the "shoulder" positions match with the positions of the two main peaks obtained in absence of diffusion quite well.

"POWDER" SAMPLE: BIPOLAR DROPLETS

In most experimental NMR studies of PDLC [2,4,14–16] bipolar droplets have been observed. In a real sample there are many droplets whose symmetry axes are oriented randomly. Macroscopically, such sample is isotropic although the constituent bipolar droplets are not. Then, since the NMR spectrum is a collective response of all droplets inside the sample, in the spectrum one should expect to see the Pake-type pattern — characteristic for isotropic orientational distributions — instead of the two-peaked spectrum obtained for a single droplet (see previous Section). In an experiment, the two-peaked spectrum can be obtained only if all bipolar symmetry axes are preliminarily aligned by a strong external electric or magnetic field.

Although we only have the MC data for one droplet available, it is possible to simulate the effect of randomly oriented droplet symmetry axes by using the unaltered single droplet data and by assuming to have a random distribution of spectrometer magnetic field directions. Since we simply "clone" the data for a single droplet to model several droplets, this certainly results in unphysical correlations between particle orientations in different droplets, but at least in cases with diffusion this should not be of great importance since interdroplet correlations are smeared out by independent diffusion paths in each droplet. Note that now spectra show much less noise than for a single droplet and it is not necessary to perform smoothening convolutions.

Fig. 4 (a) shows the spectrum of 1000 bipolar droplets without diffusion at $T^* = 0.8$ (nematic phase). It presents a Pake-type pattern, as expected, with peaks positioned at $\pm 0.37\,\delta\omega_Q$. This suggests that $S \approx 0.74$, which is close to $S \approx 0.73$, a value deduced from peak positions for a single

bipolar droplet — see Fig. 3 (a). In the spectrum, fast and homogeneous diffusion again results in a Pake-type pattern, albeit somewhat narrowed [Fig. 4 (c)]. The ratio of line widths measured peak-to-peak in cases with and without fast diffusion should be equal to that calculated for a single bipolar droplet. For a single droplet this ratio is estimated by 0.83, while for an array of 1000 droplets we have 0.80, indicating that the agreement is good.

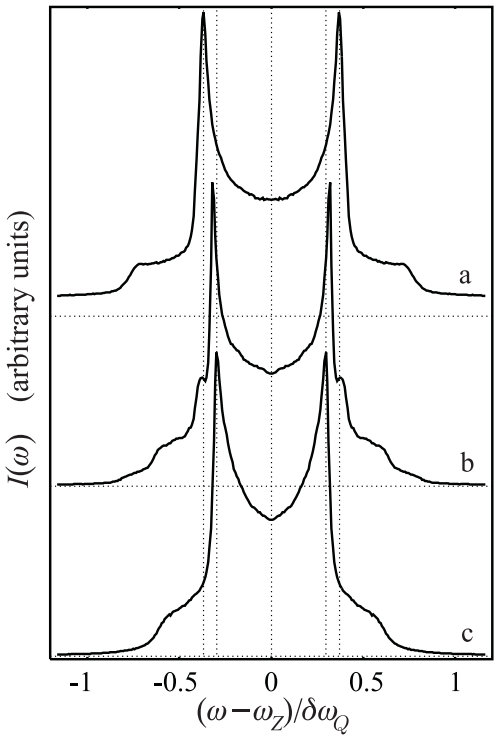

FIGURE 4 Spectra of 1000 bipolar droplets at $T^* = 0.8$, with symmetry axes oriented randomly: no diffusion (a), fast diffusion: inhomogeneous (b) and homogeneous (c).

Finally, if diffusion is inhomogeneous [Fig. 4 (b)], the spectrum is still similar to the Pake-type pattern, however, with less width reduction than in the homogeneous diffusion case. In addition, at splittings slightly larger than those corresponding to the main peaks, two "shoulders" appear again. Note that all these features agree with those observed for a single bipolar droplet; compare with Fig. 3 (b). The spectrum shown in Fig. 4 (b) actually consists of two superimposed Pake-type patterns. The first one — comprising the two main peaks — is well pronounced and originates from central droplet regions where diffusion is effective.

The two "shoulders", on the other hand, are the main peaks of the less pronounced, but not diffusion-narrowed second Pake-type pattern representing the response from droplet surface layers. Note that the "shoulder" and no-diffusion peak positions [Fig. 4 (a)] match again.

CONCLUSIONS

In this paper, we presented calculations of NMR spectra for bipolar and radial nematic droplets, starting from the numerical output of Monte Carlo simulations. Calculating the spectra, we focused on dynamic effects, especially on translational diffusion and on its slowing-down in the surface layer. If close to the confining substrate diffusion is significantly slower than in the bulk liquid crystal, this results in perceptible changes in NMR spectra. These changes should be detectable also experimentally in small enough droplets. Finally, we calculated some "powder" spectra for an array of many bipolar droplets with randomly oriented symmetry axes and found a good qualitative agreement with the expected Pake-type patterns.

Acknowledgments

C. Z. wishes to thank the University of Bologna, CNR and MURST (PRIN "Cristalli Liquidi") for support. C. C. and P. P. are grateful to INFN through the grant IS BO12. G. S. and S. Ž. acknowledge the financial support of the Ministry of Science and Technology of Slovenia (Grant No. J1-7470) and of the European Union (Project SILC TMR ERBFMRX-CT98-0209).

References

1. G. P. Crawford and S. Žumer, Liquid Crystals in Complex Geometries Formed by Polymer and Porous Networks (Taylor and Francis, London 1996).

2. A. Golemme, S. Žumer, J. W. Doane, and M. E. Neubert, Phys. Rev. A **37**, 559 (1988).

3. R. Ondris-Crawford, E. P. Boyko, B. G. Wagner, J. H. Erdmann, S. Žumer, and J. W. Doane, J. Appl. Phys. **69**, 6380 (1991).

4. R. Aloe, G. Chidichimo, and A. Golemme, Mol. Cryst. Liq. Cryst. **203**, 1155 (1991).

5. P. Pasini and C. Zannoni, Advances in the Computer Simulations of Liquid Crystals (Kluwer, Dordrecht 2000).

6. C. Chiccoli, P. Pasini, F. Semeria, E. Berggren, and C. Zannoni, Mol. Cryst. Liq. Cryst. **266**, 241 (1995).

7. E. Berggren, C. Zannoni, C. Chiccoli, P. Pasini, and F. Semeria, Phys. Rev. E **49**, 614 (1994).

8. E. Berggren, C. Zannoni, C. Chiccoli, P. Pasini, and F. Semeria, Phys. Rev. E **50**, 2929 (1994).

9. C. Chiccoli, P. Pasini, G. Skačej, C. Zannoni, and S. Žumer, Phys. Rev. E **60**, 4219 (1999).

10. C. Chiccoli, P. Pasini, G. Skačej, C. Zannoni, and S. Žumer, to appear in Phys. Rev. E **62** (2000).

11. G. P. Crawford, D. K. Yang, S. Žumer, D. Finotello, and J. W. Doane, Phys. Rev. Lett. **66**, 723 (1991).

12. M. Vilfan, G. Lahajnar, I. Zupančič, S. Žumer, R. Blinc, G. P. Crawford, and J. W. Doane, J. Chem. Phys. **103**, 8726 (1995).

13. P. A. Lebwohl and G. Lasher, Phys. Rev. A **6**, 426 (1972).

14. M. Ambrožič, P. Formoso, A. Golemme, and S. Žumer, Phys. Rev. E **56**, 1825 (1997).

15. A. Golemme, S. Žumer, D. W. Allender, and J. W. Doane, Phys. Rev. Lett. **61**, 2937 (1988).

16. J. Dolinšek, O. Jarh, M. Vilfan, S. Žumer, R. Blinc, J. W. Doane, and G. Crawford, J. Chem. Phys. **95**, 2154 (1991).

17. A. Abragam, The Principles of Nuclear Magnetism (Clarendon Press, Oxford 1961).

18. P. G. de Gennes and J. Prost, The Physics of Liquid Crystals (Clarendon Press, Oxford 1993).

19. C. Chiccoli, P. Pasini, F. Semeria, T. J. Sluckin, and C. Zannoni, J. Phys. II **5**, 427 (1995).